Light-Activation of Molecular Motors in Polymersomes

Journal:	*Molecular Systems Design & Engineering*
Manuscript ID	ME-ART-10-2023-000165.R1
Article Type:	Paper
Date Submitted by the Author:	01-Dec-2023

Complete List of Authors:	Dawn, Soumya; Louisiana State University, Chemistry Klisch, Stefanie; Louisiana State University, Chemistry Schneider, Gerald; Louisiana State University, Chemistry; Louisiana State University, Physics & Astronomy García-López, Víctor; Louisiana State University, Chemistry

Design, System, Application Statement

We have successfully engineered a molecular motor capable of rotating at an approximate frequency of 1 mHz within the bilayer of $PDMS_{11}$-*b*-PEG_{13} polymersomes and in solution. We chose hydrophobic PDMS as one of the polymersome materials to ensure the insertion of the non-polar molecular motors into the bilayer. Moreover, by utilizing a fluorenyl-based stator and a rotor featuring a five-membered ring, we reach a rotational frequency in the mHz regime, which can be conveniently monitored by UV-Vis spectrophotometry, preventing the use of more specialized techniques required for faster motors.

Furthermore, we established a synthetic protocol to obtain the motor with two methoxy groups. This will facilitate future derivatization to incorporate other moieties to control the motor's orientation, location, and interaction within the polymersome.

We speculate our observations could extend beyond the specific motor studied, so faster motors may also maintain their rotation properties in polymersomes, enabling the generation of perturbations of varying strengths in the polymersomes. Hence, we anticipate that molecular motors will play an important role in driving more complex polymersomes away from their thermodynamic equilibrium, a requirement for light-activated nanoreactors, artificial organelles and cells, and new drug delivery systems.

Light-Activation of Molecular Motors in Polymersomes

Soumya Kanti Dawn,[1]† Stefanie Klisch,[1]† Gerald J. Schneider[1,2]* Víctor García-López[1]*

[1] Department of Chemistry, Louisiana State University, Baton Rouge, LA 70803, United States
[2] Department of Physics & Astronomy, Louisiana State University, Baton Rouge, LA 70803, United States

† Contributed equally
*Corresponding authors: gjschneider@lsu.edu, vglopez@lsu.edu

Abstract

Light-activated synthetic organic molecular motors are emerging as an excellent prospect to actuate supramolecular assemblies such as polymersomes with spatiotemporal precision. The influence on these materials depends on the motor's frequency of rotation and concentration. Therefore, we determined the rotation frequency of a motor in a poly(dimethyl siloxane)-*b*-poly(ethylene glycol) ($PDMS_{11}$-*b*-PEG_{13}) polymersome and compared it to the frequency observed in different organic solvents. Using UV-Vis spectrophotometry and Nuclear Magnetic Resonance Spectroscopy, we measured the rate of the thermal helix inversion step, which is the rate-determining step of the rotary cycle, and obtained the activation parameters. We found that the investigated motor's frequency of rotation did not significantly change in the polymersomes and remains at around 1 mHz. Moreover, dynamic light scattering results indicate that the rotation of the motors does not cause a significant change in the structure of this type of polymersome when used at a diblock copolymer:motor molar ratio of up to 100:2. Our findings provide a first insight into the effect of the polymersome on the motor's frequency of rotation and vice versa. Enhancing the polymersome composition with motors can lead to novel concepts, including light-activated nanopharmaceuticals, nanoreactors, and biomimetic artificial organelles and cells.

1. Introduction

Artificial molecular motors based on overcrowded alkenes can produce mechanical work and influence their environment by transforming photonic energy into continuous cyclic molecular motion; specifically, one half of the motor rotates unidirectionally with respect to the other half around the rotation axle.[1–5] Therefore, an exciting opportunity is the incorporation of motors in polymersomes to use the motor's rotation to drive the system out of its thermodynamic equilibrium and control the permeability, lateral fluidity, size, or other physical properties. This is important because polymersomes are vesicles that have emerged as promising delivery systems for all sorts of cargo, such as small drug molecules, probes, proteins, and genetic material.[6–8] Too, polymersomes can be used as nanoreactors in enzymatic catalysis and to develop artificial organelles and cells mimicking living cellular functions.[9–11]

The advantage of using light-driven molecular motors to actuate the polymersomes instead of temperature or pH–responsive units is the possibility of controlling the system with spatiotemporal precision. Moreover, the polymersomes response could be modulated by adjusting the motor concentration and frequency of rotation; the latter can be tuned through chemical design and by changing the light intensity, irradiation time, and temperature, offering several handles to control the outcome.[1,2,12,13]

However, despite the tremendous potential opportunities, little is known about how motors behave in polymersomes. So far, there are several reports of motors that modulate or altogether disassemble lipid membranes of different compositions. For instance, motors, which in a solution can reach rotation frequencies in the MHz regime, create perturbations and permanently disrupt the lipid membrane of cancer cells[14] and antibiotic-resistant bacteria[15] when excited with intense light (>140 $mW.cm^{-2}$), causing cell death. These motors can also kill fungi by disrupting the

mitochondrial phospholipid membrane.[16] Moreover, at lower light intensities (5-60 mW.cm^{-2}), the motors rotate slower, allowing the modulation of the membrane fluidity without disassembling the bilayer, which was used to promote the transport of K^+ ions in synthetic lipid vesicles and cancer cells.[17,18] Remarkably, motors designed to rotate at lower frequencies (mHz) facilitated up to 18% of cargo release from lipid vesicles when irradiated at 0.2 mW.cm^{-2}.[19] However, in this previous study, the irradiation was done for only 30 seconds, so the observed effect could be a consequence of photoisomerization and not the continuous rotation of the motors.

Notably, polymersomes are known to be chemically and mechanically more stable than their lipid analogs, showing lower lateral fluidity and permeability and more significant resistance to deformation and stretching.[6,20] Although this overcomes the leakage problems commonly observed in liposomes, it could complicate the release of cargo for drug delivery or the internalization of substrates when used as nanoreactors. Thus, using motors to modulate the polymersome structure and dynamics with spatiotemporal precision is a promising solution to this challenge. However, this also opens the question of whether motors can rotate and induce an effect in the stiff polymersomes.

In this work, we provide new insights to answer these fundamental questions. We synthesized molecular motor **1** and studied its rotation in the bilayer of polymersomes (≈75 nm diameter) formed by the self-assembly of poly(dimethyl siloxane)-*b*-poly(ethylene glycol) ($PDMS_{11}$-*b*-PEG_{13}) diblock copolymers, which we have studied in the past (**Figure 1**).[21] We measured the rate of the thermal helix inversion step (the rate-determining step in the rotary cycle of the motor) and estimated the average frequency of rotation in solution and the polymersomes. Our data shows that, at least in the polymersomes used, molecular motors rotate at a similar frequency that in organic solvents (≈1 mHz). Moreover, at the maximum motor concentration studied ($1x10^{-4}$ mol

L^{-1}, 2 mol%), the light-triggered rotation of the motor did not cause a change in the size of the polymersomes or induce disassembly as previously observed in lipid vesicles. This helped us to discard any potential effect of polymersome disassembly in the motor's frequency of rotation.

Recently, Guinart et al. published a study showing that the light irradiation of molecular motors can cause the complete disassembly of polymersomes of $PDMS_{25}$-*b*-$PMOXA_{10}$ diblock copolymers and activate the delivery of drugs.[22] They achieved this by loading up to 50 mol% of their motor in polymersomes of ≈150 nm diameter. The authors demonstrated the first step of the motor's rotary cycle (the E/Z photoisomerization) in the polymersome, but the thermal helix inversion step was not investigated. Thus, our independent work provides new quantitative insights to demonstrate that the rate of the thermal helix inversion step and, therefore, the motor's frequency of rotation does not decrease in the bilayer of certain polymersomes.

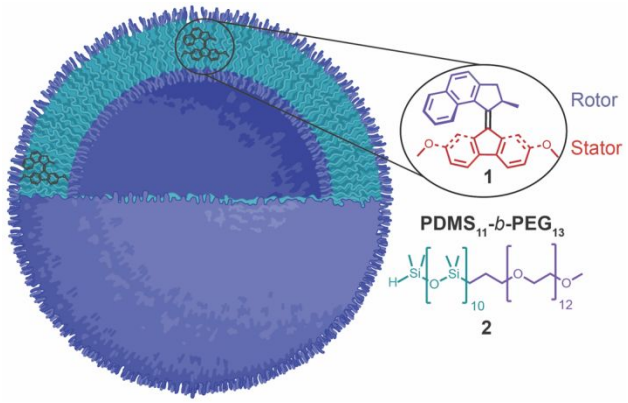

Figure 1. Molecular motor, **1**, in the hydrophobic region of the bilayer of a polymersome formed by the self-assembly of $PDMS_{11}$-*b*-PEG_{13} diblock copolymer **2.** Created with BioRender.

2. Results and discussion

Molecular design and synthesis

We designed motor **1** (**Figure 1**) with a fluorenyl–based stator and a rotor with a five-membered ring connected to the double bond to reach rotation frequencies in the mHz regime, so it is more convenient to follow its rotation by ^{1}H-NMR and UV-Vis spectroscopy. Moreover, we

designed amphiphilic diblock copolymer **2** consisting of a hydrophilic PEG chain and the highly hydrophobic PDMS unit. Thus, the non-polar motors are expected to be inserted into the PDMS region of the bilayer.

The synthesis of the motors started with the preparation of the stator. First, commercially available 2,7-dihydroxy-9-fluorenone (**3**) was methylated to protect the phenol groups and form **4** (**Scheme 1**). Then, a thiation reaction produced thioketone **5**, which reacted with hydrazine monohydrate for one hour to give hydrazone **6** in good yield. We also attempted another route for the synthesis of hydrazone **6** by instead reacting ketone **4** with hydrazine monohydrate, but the reaction took 21 hours. Lastly, we carried out a two-step Barton-Kellogg olefination process between the stator hydrazone **6** and previously reported rotor thioketone **7**[23] to obtain motor **1**.

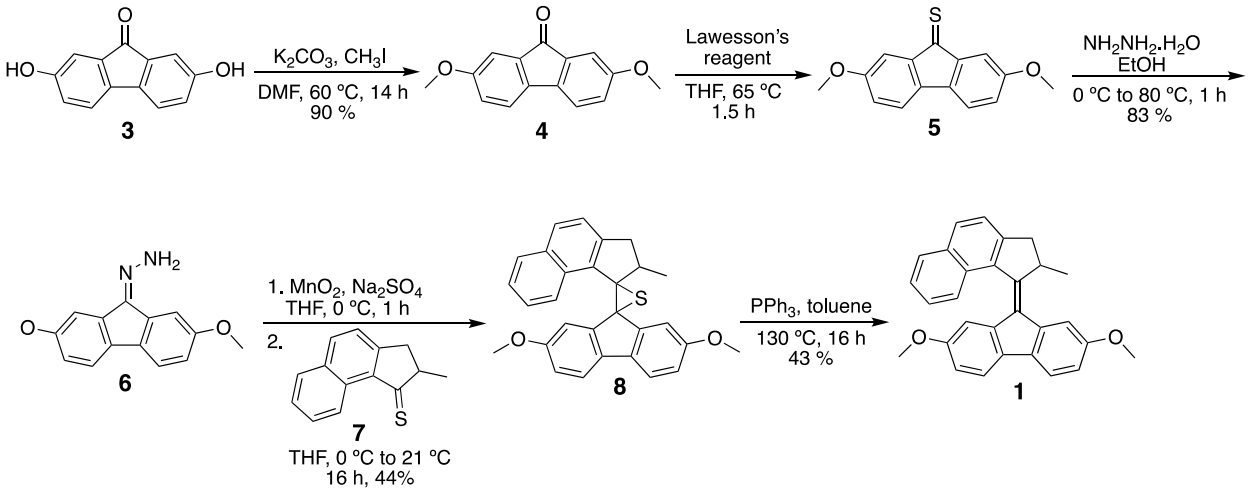

Scheme 1. Synthesis of motor. a) synthesis of stator **6**, and b) Barton–Kellogg reaction to obtain motor **1**.

Diblock copolymer **2** was synthesized through a catalytic hydrosilylation reaction between alkene–functionalized PEG_{13} (**9**) and $PDMS_{11}$ (**10**) (**Scheme 2**).[21] The formation of the diblock copolymer was monitored by following the disappearance of the vinylic proton peaks of the PEG

group in the ^{1}H NMR spectrum (**Figure S1**). Moreover, high-resolution MALDI-MS was used to confirm the formation of diblock copolymer **2** (**Figure S2**).

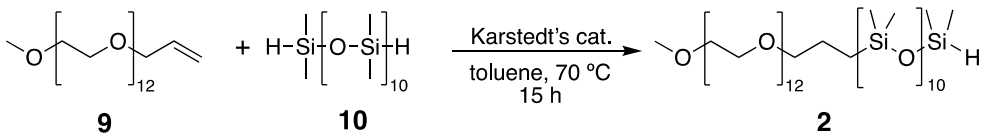

9 **10** **2**

Scheme 2. Synthesis of diblock copolymer **2**.

Probing the rotation of molecular motor 1 in solution

Each motor rotation proceeds as a four-step cycle comprised of two fast photoisomerization steps (picoseconds) and two much slower thermal helix inversions (THIs) (**Figure 2a**).[1,2,12] At the initial motor **1a**, the methyl group in the upper half (rotor) is in a pseudo-axial conformation to minimize steric repulsion with the lower half of the molecule (see crystal structure, **Figure S4**). Upon irradiation with light, photoisomerization around the alkene bond occurs, forming the metastable isomer **1b**, which is higher in energy. This photoisomerization inverts the molecule's helicity, and the methyl group now adopts a strained pseudo-equatorial orientation, experiencing steric crowding with the lower half. The next step in the cycle is an energetic downhill thermal helix inversion that forms stable isomer **1c**. This unidirectional step releases the strain and allows the methyl substituent to adopt the more stable pseudo-axial orientation, completing half of the cycle. The subsequent step is a second photoisomerization to form **1d**, followed by a second unidirectional thermal helix inversion that regenerates **1a**.

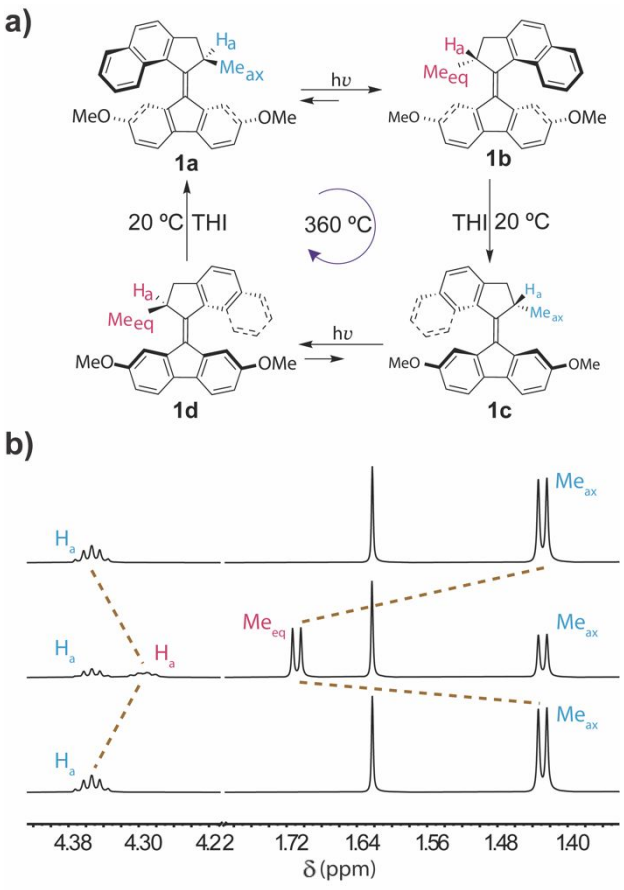

Figure 2. a) Four steps rotary cycle of motor **1**. b) Partial ^{1}H NMR spectra of motor **1a** in chloroform-*d* before irradiation (bottom), after irradiation showing the formation of metastable **1b** (middle), and after 30 min in the dark at 20 °C showing the completion of the THI and formation of **1c** (top). The full spectra are shown in **Figure S5.**

Reported motors similar to the one we studied (**1**) have a frequency of rotation between 0.4 and 1.8 mHz in solution. Specifically, the metastable isomers have a half-life ($t_{1/2}$) between 192 – 900 s at 20 °C, resulting in thermal helix inversions with rates (k) between $1.4\text{x}10^{-3}$ – $3.6\text{x}10^{-3}$ s^{-1} depending on the solvent and chemical structure of the motor.[24–27] Thus, the THI is several orders of magnitude slower than the photoisomerizations (picoseconds), so it is accepted only to consider the THI rate when estimating the rotation frequency.[1,2,12,24–27]

We first studied the rotation of **1** in solution by ^{1}H NMR spectroscopy. We irradiated motor **1a** dissolved in chloroform-*d* at 370 nm for 10 minutes at –20 °C outside the NMR instrument to

slow down the THI and trap a fraction of the metastable isomer **1b**. The chemical shift of the methyl group moved downfield from 1.42 ppm to 1.71 ppm, indicating the formation of **1b** and in agreement with the observed changes for other motors (**Figure 2b**).[1,24,26] Although the irradiation was done at –20 °C, the NMR measurement was carried out at 20 °C, partially allowing the THI; thus, we obtained a 48:52 (**1b**:**1c**) ratio. We then monitored the disappearance of the peak at 1.71 ppm in 90 s intervals and observed full completion of the thermal helix inversion in less than 30 min (**Figures 2b**, **3a,** and **Figures S6-S7**).

By plotting the natural logarithm of the concentration of **1b** vs. time, we obtained the characteristic first-order kinetics for the monomolecular thermal helix inversion (**Figure 3b**). We measured a rate constant (k) of 0.00205 s^{-1} and a half-life ($t_{1/2}$) of 338 s for the THI of **1b** (**Table 1**). Because of the symmetry of our stator, the two THIs are equivalents and occur at the same rate. Therefore, we can determine the frequency of rotation by dividing the rate constant by two,[1,25] so motor **1** was found to have a frequency of rotation of 1.0 mHz in chloroform-*d* at 20 °C, which is consistent with the values measured for similar motors at the same temperature.[24,25] Furthermore, we also followed the THI at other temperatures (5 °C, 10 °C, and 15 °C), and using Eyring analysis (**Figures S8-S9**), we determined the standard values of the thermodynamic parameters for the thermal helix inversion ($\Delta^{\ddagger}G°$, $\Delta^{\ddagger}H°$, and $\Delta^{\ddagger}S°$), which are summarized in **Table S2**.

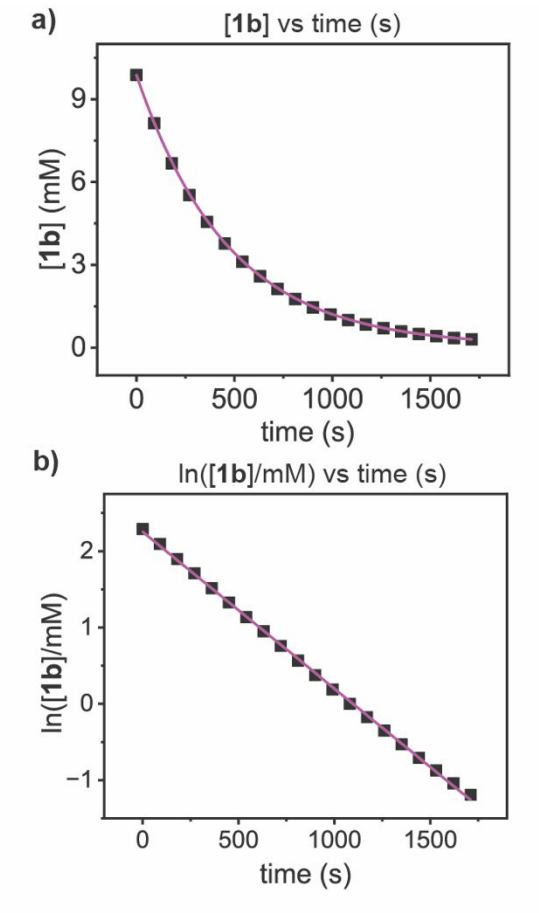

Figure 3. (a) Decrease in the concentration of metastable **1b** over time measured by ^{1}H NMR spectroscopy in chloroform-*d*. (b) First-order kinetic analysis of the NMR data. The slope of the linear fit gives the THI rate constant (k) of 0.00205 s^{-1} at 20 °C.

Similarly, the kinetic parameters of THI of motor **1** were also measured in acetone-d_6 by ^{1}H NMR (**Figure S10**). We found the motor has a frequency of rotation of 1.3 mHz in this solvent (**Table 1**). Nevertheless, ^{1}H NMR spectroscopy could not be used to study the motor's rotation in the polymersomes because of the motor's low signal-to-noise ratio and overlap with the copolymer signals.

Furthermore, we first established a protocol to measure the THI rate constant in different solvents (acetone and chloroform) by UV-Vis spectrophotometry and compare it to results obtained by ^{1}H NMR. The samples were irradiated at 370 nm for 5 minutes at 21 °C, resulting in a red shift in the absorbance spectrum, which is assigned to the metastable isomer **1b** (λ_{max}= 413

nm) and is consistent with what is reported in the literature for similar motors.[25,26] Then, we followed the disappearance of **1b** over time until complete conversion to isomer **1c** (λ_{max}= 387 nm). The kinetic parameters were determined by a fit of the data obtained from the UV-Vis absorption peaks with a Gaussian distribution function, summarized in **Table 1** (Gaussian fit is explained in supporting information **Section S7.1** and **Figure S11**). We found a half-life ($t_{1/2}$) of motor **1** in acetone and chloroform of 237 s and 404 s, respectively (**Figure 4**), corresponding to rotation frequencies of 1.4 and 0.8 mHz, respectively, in agreement with the NMR data.

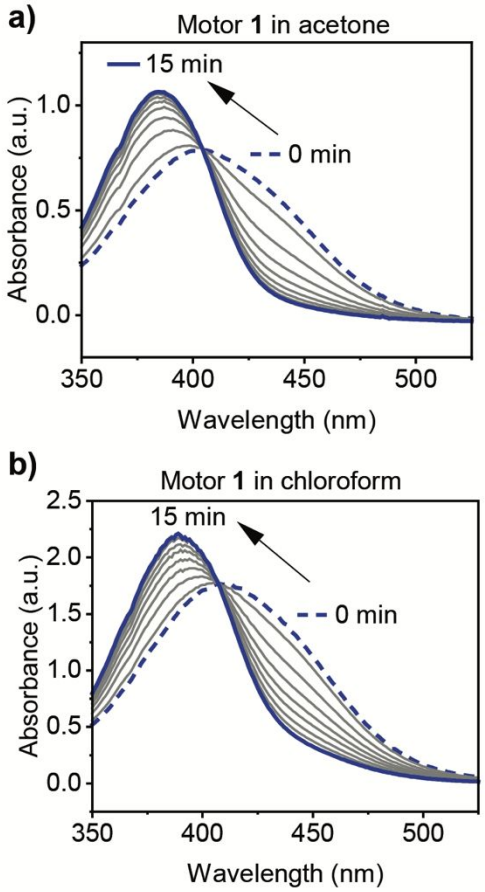

Figure 4. UV-Vis absorption spectra showing the thermal helix inversion from metastable **1b** to stable **1c** over time in (a) acetone and (b) chloroform. Metastable **1b** (dash line) was formed after irradiation with 370 nm for 5 min. Over time, **1b** converts into **1c** (solid line). 1 x10^{-4} mol L^{-1} of the motor was dissolved in each solvent.

Table 1. Kinetic parameters of the thermal helix inversion (THI) in solution and in polymersome.

Sample	ω (mHz)	k ($s^{-1}x10^{-5}$)	$t_{1/2}$ (s)	Method
Acetone-d_6	1.3	265 ± 1	261 ± 1	NMR
Acetone	1.4	270 ± 5	237 ± 4	UV-Vis
Chloroform-*d*	1.0	205 ± 1	338 ± 1	NMR
Chloroform	0.8	158 ± 1	404 ± 2	UV-Vis
Polymersome	0.9	178 ± 1	360 ± 3	UV-Vis

ω = frequency of rotation of the motor, k = rate constant for the THI, $t_{1/2}$ = half-life for the THI. Temperature = 20 °C for NMR data and 21 °C for UV-Vis spectrophotometry.

Polymersomes preparation and characterization without light irradiation

Having studied the rotary properties of motor **1** in different solvents by different techniques, we then proceeded to prepare polymersomes with different amounts of motor **1** embedded in the hydrophobic region. For this, we modified a thin film hydration procedure previously reported by us (Supporting Information, **Section S3**).[21] Specifically, we prepared polymersomes with diblock copolymer:motor molar ratios of 100:0, 100:0.5, 100:1, and 100:2.

In order to obtain visual information of the polymersome samples, a Cryo-TEM image of the polymersomes incorporated with motor **1** was taken (**Figure 5**), offering a good first impression and showing that the polymersomes have the characteristic vesicle structure. Moreover, to investigate the system in a more natural environment, we used dynamic light scattering spectroscopy (DLS) to measure the hydrodynamic diameter (D_H) and polydispersity index (PDI) in solution. We found that the incorporation of the motors at these concentrations does not have a significant effect on the D_H and PDI, and the polymersomes have an average D_H of 75 ± 1 and PDI of 0.20 ± 0.02 (**Table 2** and **Figure 6**). The average was calculated from three measurements for each molar proportion, and the error displayed represents the standard deviation.

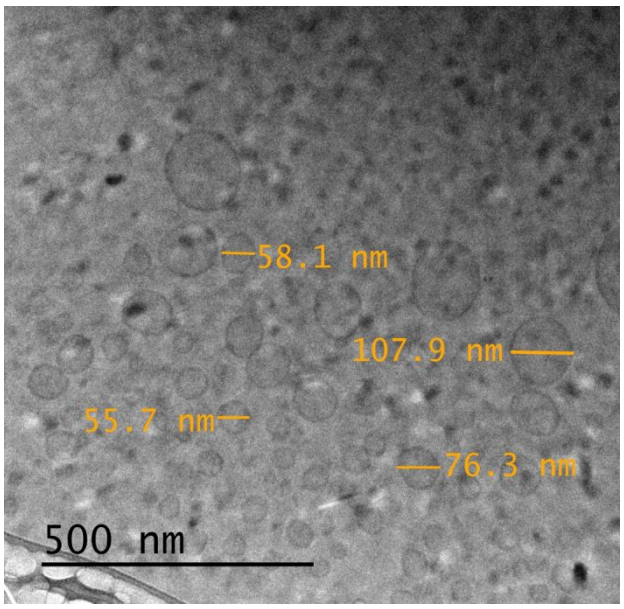

Figure 5. Cryo-TEM image of the polymersomes with diblock copolymer:motor ratios of 100:2.

Table 2. Average hydrodynamic diameter (D_H) and polydispersity index (PDI) of polymersomes incorporated with different concentrations of motor **1** without light irradiation at 22 °C.

Diblock copolymer:motor molar ratio	**D_H (nm)**	**PDI**
100:0	74.6 ± 0.4	0.19 ± 0.01
100:0.5	75.8 ± 0.8	0.24 ± 0.00
100:1	75.7 ± 0.5	0.19 ± 0.01
100:2	74.3 ± 0.5	0.2 ± 0.01

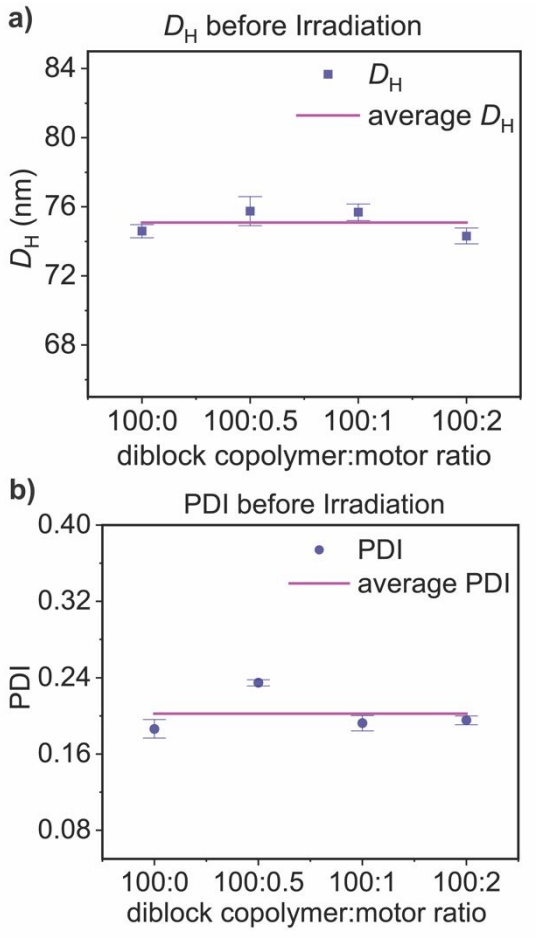

Figure 6. a) Hydrodynamic parameter (D_H) and b) polydispersity index (PDI) of polymersomes with different concentrations of motors without light irradiation. DLS measurements were collected at 22 °C.

Probing the rotation of the motor in the polymersomes upon light activation

We then investigated the influence of motor activation on the polymersome structure upon light irradiation. The samples were irradiated at 370 nm for 5 minutes and then inserted into the DLS instrument in less than 1 minute for measurements over 15 minutes at 24 °C. As can be seen from **Table 3** and **Figure 7**, we observed a diameter D_H and PDI that do not seem to depend on the irradiation; all D_H values fall within 1 nm from the average D_H value for each motor loading. Furthermore, calculating the average diameter and PDI shows that the results randomly scatter around these values. Thus, we conclude within the accuracy of our experimental data that there is

no systematic dependence on the irradiation, and the motor activation under these conditions does not alter the physical properties of the polymersomes.

Table 3. Average hydrodynamic diameter (D_H) and polydispersity index (PDI) of polymersomes incorporated with different concentrations of motor **1** after 5 min of light irradiation at 24 °C.

Diblock copolymer:motor molar ratio	$\boldsymbol{D_H}$ (nm)	**PDI**
100:0	74.7 ± 0.5	0.19 ± 0.02
100:0.5	73.6 ± 0.6	0.20 ± 0.01
100:1	75.8 ± 0.6	0.19 ± 0.01
100:2	74.2 ± 0.6	0.19 ± 0.02

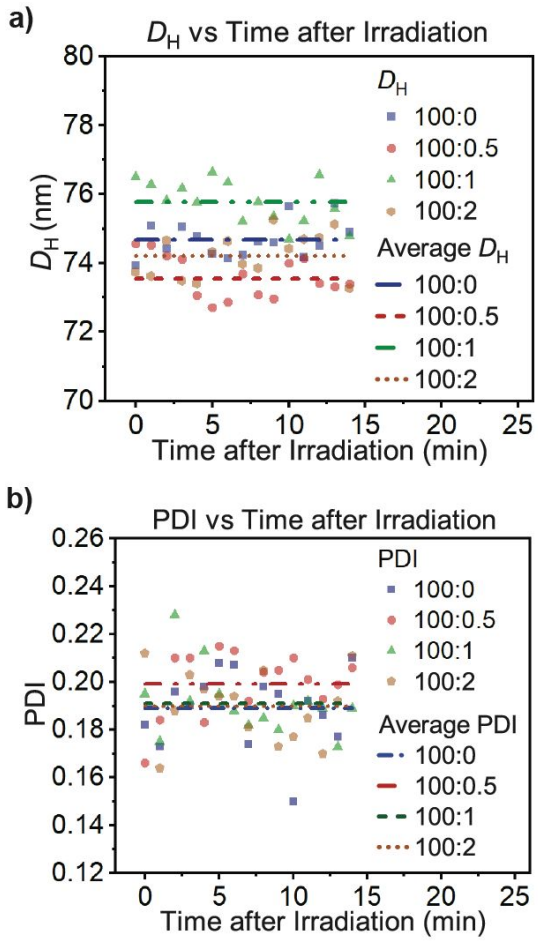

Figure 7. a) Hydrodynamic diameter (D_H) and b) polydispersity index (PDI) of the polymersomes with different amounts of motors after 5 min of light irradiation at 24 °C. Cumulant fit error bars are smaller than the symbol size and were omitted for clarity.

Moreover, we tested the stability of our polymersomes upon being stored for 13 days at the ambient temperature of our laboratory (22 °C) and in the dark. As **Figure 8** shows, there were no changes in their diameter or polydispersity, regardless of motor concentration.

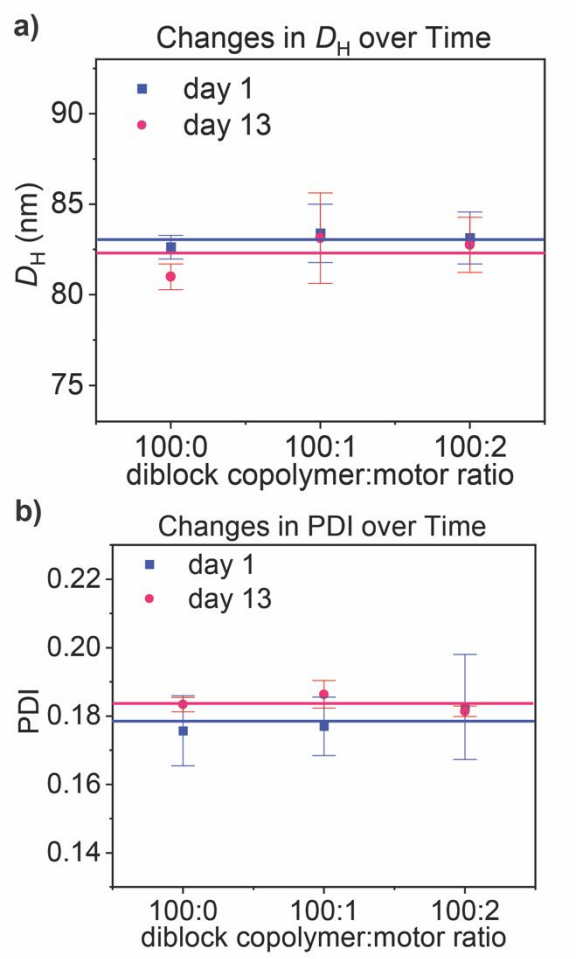

Figure 8. a) D_H and b) PDI for polymersomes after 13 days of storage in the dark at 22 °C.

Lastly, we then determined the kinetics of the thermal helix inversion of the motors in the polymersome bilayers by UV-Vis spectrophotometry. The samples were irradiated at 370 nm for 5 minutes to generate the metastable isomer **1b** (λ_{max}=415 nm), then, we followed the formation of the stable **1c** (λ_{max}= 387 nm) over time (**Figure 9**). The kinetic parameters were obtained by the Gaussian distribution fit of the UV-Vis peaks (**Table 1,** Supporting information **Section S7**). The data shows that the rate of the THI is comparable to the ones measured in solution. Thus, the motor

rotates at ≈0.9 mHz in the polymersomes, indicating that the rotary behavior is conserved in the bilayer. This could mean that the $PDMS_{11}$-*b*-PEG_{13} diblock copolymers are flexible enough to allow the conformational changes of motor **1** in the polymersomes.

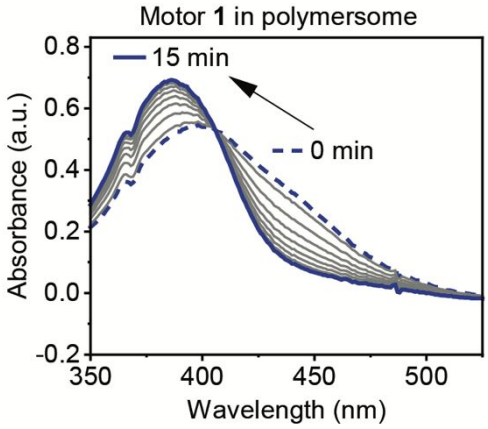

Figure 9. UV-vis absorption spectra showing the thermal helix inversion of motor **1** incorporated in polymersomes. Metastable **1b** (dash line) was formed after irradiation with 370 nm for 5 min. Over time, **1b** converts into **1c** (solid line).

3. Conclusions

Our study provides quantitative data demonstrating that, when activated with light, a molecular motor rotates in the bilayer of $PDMS_{11}$-*b*-PEG_{13} polymersomes at a similar frequency as in solution—indicating that at least this type of diblock copolymer assembly exerts a minimum effect on the rotary behavior of the motors. Moreover, at the low motor loadings used in this study (<2 mol%), the light-triggered rotation of the motors does not alter the structure of the polymersomes. However, the recent results reported by Guinart show that at much larger concentrations (50 mol%), the rotation of a motor can induce the disassembly of larger polymersomes ($PDMS_{25}$-*b*-$PMOXA_{10}$).[22]

Therefore, we can establish the following paradigms: (1) molecular motors can rotate in PDMS-*b*-PEG type polymersomes similarly as in solution, and (2) the effect of the motor rotation

on the polymersomes depends on the motor concentration, light intensity, time of irradiation, polymersome size, and chemical properties of the diblock copolymer.

We envision that our findings will encourage future studies where motors of different rotation speeds activated with visible[28,29] or near-infrared light[30,31] modulate more complex polymersomes, resulting not only in new delivery systems for therapeutic and theranostic applications but also in new light-activated nanoreactors, and out-of-equilibrium artificial cells and organelles.

Conflict of Interest

The authors declare the following competing financial interest(s): V.G.L. is a co-inventor of a patent for using molecular motors to destroy cells for medical treatments. The IP has been licensed to a company in which V.G.L. has no role or participation. Conflicts of interest are mitigated through regular disclosure to the Louisiana State University office of research and economic development. The authors declare no other potential conflict of interest.

Acknowledgments

We thank Dr. Frank Fronczek for collecting and analyzing the X-ray crystallographic data. V.G.L holds a Career Award at the scientific interface from the Burroughs Wellcome Fund. Also, this material is based upon work supported by the National Science Foundation under Award No. OIA-1946231; any opinions, findings, conclusions, or recommendations expressed in this material are those of the author(s) and do not necessarily reflect the views of the National Science Foundation. We acknowledge the Shared Instrumentation Facility of Louisiana State University for collecting the CryoTEM images in support of this research.

Author Contributions

Soumya K. Dawn: Methodology, Validation, Formal Analysis, Investigation, Writing – Original Draft, Visualization. **Stefanie Klisch:** Methodology, Validation, Formal Analysis, Investigation, Writing – Original Draft, Visualization. **Gerald Schneider:** Conceptualization, Writing – Review & Editing, Supervision, Project administration, Funding acquisition. **Víctor García-López**: Conceptualization, Methodology, Writing – Original Draft, Writing – Review & Editing, Visualization, Supervision, Project administration, Funding acquisition.

References

1 V. García-López, D. Liu and J. M. Tour, *Chem. Rev.*, 2020, **120**, 79–124.

2 D. Roke, S. J. Wezenberg and B. L. Feringa, *Proc. Natl. Acad. Sci. U.S.A.*, 2018, **115**, 9423–9431.

3 S. Zhang, Y. An, X. Chen, I. Aprahamian and Q. Li, *Responsive Mater.,* 2023, e20230023.

4 H. Wang, H. K. Bisoyi, X. Zhang, F. Hassan and Q. Li, *Chem. Eur. J.,* 2022, **28**, 2202103906.

5 L. Wang and Q. Li, *chem. Soc. Rev.,* 2018, **47**, 1044–1097.

6 J. Lefley, C. Waldron and C. R. Becer, *Polym. Chem.*, 2020, **11**, 7124–7136.

7 J. H. Lam, A. K. Khan, T. A. Cornell, T. W. Chia, R. J. Dress, W. W. W. Yeow, N. K. Mohd-Ismail, S. Venkataraman, K. T. Ng, Y.-J. Tan, D. E. Anderson, F. Ginhoux and M. Nallani, *ACS Nano*, 2021, **15**, 15754–15770.

8 J. S. Lee and J. Feijen, *J. Control Release*, 2012, **161**, 473–483.

9 H. Che and J. C. M. van Hest, *ChemNanoMat*, 2019, **5**, 1092–1109.

10 C. Martino, S.-H. Kim, L. Horsfall, A. Abbaspourrad, S. J. Rosser, J. Cooper and D. A. Weitz, *Angew. Chem.*, 2012, **124**, 6522–6526.

11 H. Seo and H. Lee, *Nat. Commun.*, 2022, **13**, 5179.

12 D. R. S. Pooler, A. S. Lubbe, S. Crespi and B. L. Feringa, *Chem. Sci.*, 2021, **12**, 14964–14986.

13 M. Klok, W. R. Browne and B. L. Feringa, *Phys. Chem. Chem. Phys.*, 2009, **11**, 9124.

14 V. García-López, F. Chen, L. G. Nilewski, G. Duret, A. Aliyan, A. B. Kolomeisky, J. T. Robinson, G. Wang, R. Pal and J. M. Tour, *Nature*, 2017, **548**, 567–572.

15 A. L. Santos, D. Liu, A. K. Reed, A. M. Wyderka, A. Van Venrooy, J. T. Li, V. D. Li, M. Misiura, O. Samoylova, J. L. Beckham, C. Ayala-Orozco, A. B. Kolomeisky, L. B. Alemany, A. Oliver, G. P. Tegos and J. M. Tour, *Sci. Adv.*, 2022, **8**, eabm2055.

16 A. L. Santos, J. L. Beckham, D. Liu, G. Li, A. Van Venrooy, A. Oliver, G. P. Tegos and J. M. Tour, *Adv. Sci.*, 2023, **10**, 2205781.

17 H. Yang, J. Yi, S. Pang, K. Ye, Z. Ye, Q. Duan, Z. Yan, C. Lian, Y. Yang, L. Zhu, D. Qu and C. Bao, *Angew. Chem. Int. Ed.*, DOI:10.1002/anie.202204605.

18 W.-Z. Wang, L.-B. Huang, S.-P. Zheng, E. Moulin, O. Gavat, M. Barboiu and N. Giuseppone, *J. Am. Chem. Soc.*, 2021, **143**, 15653–15660.

19 L. Ribovski, Q. Zhou, J. Chen, B. L. Feringa, P. Van Rijn and I. S. Zuhorn, *Chem. Commun.*, 2020, **56**, 8774–8777.

20 E. Rideau, R. Dimova, P. Schwille, F. R. Wurm and K. Landfester, *Chem. Soc. Rev.*, 2018, **47**, 8572–8610.

21 R. M. Perera, S. Gupta, T. Li, M. Bleuel, K. Hong and G. J. Schneider, *Soft Matter*, 2021, **17**, 4452–4463.

22 A. Guinart, M. Korpidou, D. Doellerer, G. Pacella, M. C. A. Stuart, I. A. Dinu, G. Portale, C. Palivan and B. L. Feringa, *Proc. Natl. Acad. Sci.*, 2023, **120**, e2301279120.

23 D. J. Dijken, J. Chen, M. C. A. Stuart, L. Hou and B. L. Feringa, *J. Am. Chem. Soc.*, 2016, **138**, 660–669.

24 M. M. Pollard, P. V. Wesenhagen, D. Pijper and B. L. Feringa, *Org. Biomol. Chem.*, 2008, **6**, 1605.

25 J. Vicario, A. Meetsma and B. L. Feringa, *Chem. Commun.*, 2005, 5910.

26 A. Van Venrooy, A. M. Wyderka, V. García-López, L. B. Alemany, A. A. Martí and J. M. Tour, *J. Org. Chem.*, 2023, **88**, 762–770.

27 J. Conyard, P. Stacko, J. Chen, S. McDonagh, C. R. Hall, S. P. Laptenok, W. R. Browne, B. L. Feringa and S. R. Meech, *J. Phys. Chem. A*, 2017, **121**, 2138–2150.

28 L. Pfeifer, M. Scherübl, M. Fellert, W. Danowski, J. Cheng, J. Pol and B. L. Feringa, *Chem. Sci.*, 2019, **10**, 8768–8773.

29 A. Cnossen, L. Hou, M. M. Pollard, P. V. Wesenhagen, W. R. Browne and B. L. Feringa, *J. Am. Chem. Soc.*, 2012, **134**, 17613–17619.

30 L. Pfeifer, N. V. Hoang, M. Scherübl, M. S. Pshenichnikov and B. L. Feringa, *Sci. Adv.*, 2020, **6**, eabb6165.

31 D. Liu, V. García-López, R. S. Gunasekera, L. Greer Nilewski, L. B. Alemany, A. Aliyan, T. Jin, G. Wang, J. M. Tour and R. Pal, *ACS Nano*, 2019, **13**, 6813–6823.